Dimer rotation on the carbon-induced Si(001)-$c(4\times4)$ structure

G. W. Peng,[1] Y. Y. Sun,[1] A. C. H. Huan,[2,3] and Y. P. Feng[1,*]
[1]*Department of Physics, National University of Singapore, 2 Science Drive 3, Singapore 117542*
[2]*Institute of Materials Research & Engineering, 3 Research Link, Singapore 117602*
[3]*Division of Physics and Applied Physics, Nanyang Technological University, 1 Nanyang Walk, Singapore 637616*
(Received 16 June 2006; published 5 September 2006)

We present first-principles results identifying the reaction pathways for Si dimer rotations on the carbon-induced Si(001)-$c(4\times4)$ surface. The nudged elastic band calculations show that the recently proposed rotated dimer model [Phys. Rev. Lett. **94**, 076102 (2005)] can be obtained from the refined missing dimer model by dimer rotation with small energy barriers. It is found that the energy barrier is sensitive to the rotation directions of Si dimers. The energy barrier along the minimum energy path (MEP) is 0.82 eV. Three stable configurations are identified along the MEP, one of which with a single rotated dimer is more stable than all existing models and its energy is lower than that of the rotated dimer model, the previously most stable structure, by 0.25 eV per $c(4\times4)$ cell. The stabilization mechanism of the new stable structure is analyzed. We propose a possible method to search for new stable structures based on the existing models by mapping out the reaction paths in the phase configuration.

DOI: 10.1103/PhysRevB.74.115302 PACS number(s): 68.35.Fx, 68.35.Md, 68.35.Dv, 71.15.−m

I. INTRODUCTION

Carbon incorporation into a Si substrate is of great importance in developing high-performance Si-based heterostructures with tailored electronic properties. Unfortunately, due to the large lattice mismatch between Si and C, the solubility of C in bulk Si is extremely low ($\approx10^{-5}$) under a thermodynamic equilibrium, which is an obstacle to such applications. Nonequilibrium methods such as molecular-beam epitaxy can be used to overcome this obstacle and enhance the solubility up to 20% without giving rise to SiC precipitation.[1] The increased solubility results from two factors: the presence of the surface and a stress field associated with the atomic reconstruction near the surface.[2] The former can partially relieve the stress associated with the atomic size mismatch between C and Si, while the latter can couple with the impurity stress resulting in certain sites energetically favorable for C atoms.

The incorporated C, on the other hand, can modify the periodicity of the Si(001) surface significantly. It is demonstrated that the Si(001)-$p(2\times1)$ surface changes to the $2\times n$ reconstruction at low C coverage,[3] while the $c(4\times4)$ phase appears at increased C coverage.[4] The $c(4\times4)$ phase has been extensively studied for decades since its discovery.[5] It has been reported that this reconstruction can be observed in a variety of experimental conditions.[5–13] It is argued in early work that the $c(4\times4)$ phase does not contain any foreign atoms but is one of the intrinsic reconstructions.[7] However, the idea that the $c(4\times4)$ reconstruction is carbon-related is generally accepted in recent studies,[13–21] despite the discrepancy on whether the carbons are basic ingredients of the $c(4\times4)$ structure[14–20] or just provide global strain to induce the $c(4\times4)$ phase.[13,21] Recently, Kim *et al.*[3] have observed that the Si(001) exposed to C_2H_2 shows the $2\times n$ superstructure when the C concentration is below 0.05 monolayer (ML). The $2\times n$ reconstruction has been assigned to the so-called DV41 defect, where the incorporated C atoms occupy the substitutional fourth layer sites directly below Si dimers (α sites) and Si dimer vacancies directly above the incorporated C are induced. After the C concentration increases up to 0.12 ML, the $c(4\times4)$ reconstruction appears.[4] The $c(4\times4)$ phase has been assigned to the rotated dimer model (2RD) according to the combined study of scanning tunneling microscopy (STM) and density functional theory calculations. The 2RD model could be obtained from a DV41 defect in a $c(4\times4)$ cell (also referred to as the refined missing dimer model[12]) by rotating the two side Si dimers by 90°. The 2RD model in a $c(4\times4)$ unit cell contains $\frac{1}{8}$ ML C at the α site in the fourth layer. Based on the fact that the DV41 defect is energetically more favorable than the 2RD model at low C coverage ($\frac{1}{16}$ ML), while the energy ordering is reversed at high C coverage ($\frac{1}{8}$ ML), it is suggested that the dimer rotation in the $c(4\times4)$ phase helps to relieve the increased tensile stress due to the $\times4$ arranged C atoms along dimer rows.[4] To understand the process of dimer rotation and consequent surface structure transformation, a detailed knowledge of the kinetics of dimer rotation is highly desirable.

In this study, we perform first-principles calculations to identify the reaction pathways for the Si dimer rotation on the C-induced Si(001)-$c(4\times4)$ surface. We investigate how dimers rotate in passing from the refined missing dimer model (rMD) to the 2RD model. Our calculations show that the activation energies from the rMD model to the 2RD model are sensitive to the directions of rotation of Si dimers. It is found that the minimum energy path of the dimer rotation goes through three stable configurations, one of which with a single rotated dimer is more stable than all existing models and its energy is lower than that of the 2RD model, the previously most stable structure, by 0.25 eV per $c(4\times4)$ cell. The stabilization mechanism of the new stable structure is analyzed and the ordering of the new structure in a larger $c(8\times8)$ supercell is also investigated. Finally, a possible method of searching for new stable structures by nudged elastic band calculations is discussed.

II. METHODOLOGY

All calculations were performed using Vienna *ab initio* Simulation Package (VASP) (Refs. 22 and 23) based on density functional theory. The ultrasoft pseudopotentials[24] were used for electron-ion interactions and the generalized gradient approximation of Perdew and Wang[25] was used to describe the exchange-correlation functional. The electron wave function was expanded using plane waves with a cutoff energy of 300 eV. The Si(001)-$c(4\times4)$ surface was modeled by a slab geometry with ten Si atomic layers and an 11 Å vacuum. The dangling bonds of Si atoms at the bottom of the slab were terminated with hydrogen atoms. The theoretical Si lattice constant a_0=5.46 Å was used for the Si slab. The Si atoms in the bottom two Si layers and the H atoms were frozen during the relaxation to mimic the bulk. We used $2\times2\times1$ k-point mesh to sample the Brillouin zone based on the Monkhorst-Pack scheme.[26] All atoms except for the fixed ones are fully relaxed until the Hellmann-Feynman forces are smaller than 0.02 eV/Å. The climbing image nudged elastic band method (NEB) (Refs. 27 and 28) was utilized to identify possible reaction pathways for Si dimer rotations.

III. RESULTS AND DISCUSSION

A. Structural models

We first performed total energy calculations for different Si(001)-$c(4\times4)$ structural models with $\frac{1}{8}$ ML carbon per unit cell. The C atom was incorporated into the substitutional fourth subsurface layer site below a Si dimer, the α site, which is under compressive stress and therefore suitable for the smaller carbon atom.[2] The Si dimer directly above the C atom was removed to construct the rMD model (see Fig. 1). Note that in the optimized rMD model (see the side view of rMD in the inset of Fig. 1), all three dimers tilt along the same direction rather than buckle alternately, with an energy gain of 0.59 eV in our calculation. If the middle Si dimer in the rMD model was removed, we obtained the rMD_β model. The 2RD (see Fig. 1) and $\mathrm{2RD}_\beta$ models can be obtained by rotating the two side Si dimers by 90° in rMD and rMD_β, respectively. All structural models were fully relaxed, and the difference between surface energies of two models was calculated according to

$$\Delta E = (E_{\mathrm{tot}}^{\mathrm{A}} - E_{\mathrm{tot}}^{\mathrm{B}}) - (n_{\mathrm{Si}}^{\mathrm{A}} - n_{\mathrm{Si}}^{\mathrm{B}})\mu_{\mathrm{Si}}, \quad (1)$$

where $E_{\mathrm{tot}}^{\mathrm{A}}$ is the total energy of model A containing n_{Si} silicon atoms and μ_{Si} is the chemical potential of Si, which is taken to be the energy of bulk Si. Our calculations show that the 2RD model is the most stable among the four models mentioned above. The rMD and rMD_β models are less stable than the 2RD model by 0.13 and 0.79 eV per $c(4\times4)$ cell, respectively. The surface energy of the $\mathrm{2RD}_\beta$ model is slightly higher (0.06 eV) than that of the 2RD model. These results are in good agreement with the earlier DFT calculations,[4] which are listed in Table I for comparison.

B. Kinetics of dimer rotation

The transformation from the rMD model to the 2RD model involves dimer rotation, which is believed to occur in order to relieve the tensile stress due to the $\times4$ arranged C atoms along dimer rows.[4] To understand the process of the dimer rotation and how the surface structure transformation occurs, we proceed to investigate the kinetics of the dimer rotation on the C-induced Si(001)-$c(4\times4)$ surface. As shown in Fig. 1, the initial state rMD can change to the final state 2RD by rotating the two side Si dimers via three different paths: (i) two side Si dimers rotate toward the middle dimer by 90° (Path I); (ii) both side Si dimers rotate away from the middle dimer by 90° (Path II); and (iii) one side Si dimer rotates toward but the other away from the middle dimer by 90° (Path III). Note that the rotation direction indicated here is always taken to the relative position between the lower Si atom of the side dimer and the middle dimer

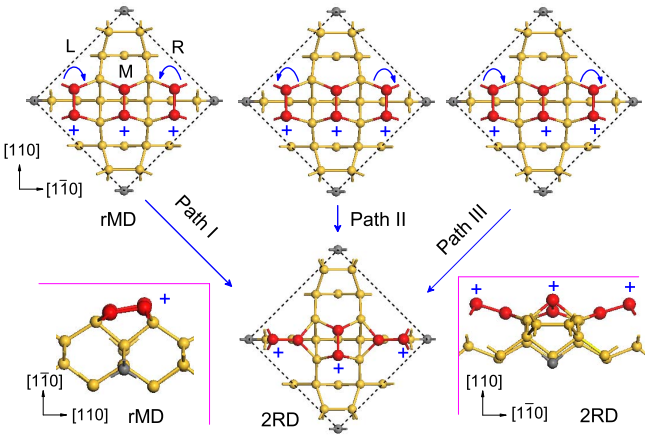

FIG. 1. (Color online) Possible pathways for the Si dimer rotations on the C-induced Si(001)-$c(4\times4)$ surface for transferring the rMD model to the 2RD model. The higher atom of a Si dimer is indicated by a plus sign if the height difference between the higher atom and the lower one is larger than 0.2 Å. The two side Si dimers can rotate toward the middle dimer by 90° (Path I); away from the middle dimer by 90° (Path II); and one toward but the other away from the middle dimer by 90° (Path III). The rotation directions are indicated by the arrows. The left and right insets are the side views of the optimized rMD and 2RD models, respectively. The Si dimer atoms, the remaining Si atoms, and the C atoms are denoted by red (dark), yellow (light), and gray spheres, respectively. The three Si dimers are categorized as left dimer (L), middle dimer (M), and right dimer (R) for distinction in the reaction processes.

TABLE I. Calculated relative surface energies per $c(4\times4)$ unit cell (in eV) for different C-induced Si(001)-$c(4\times4)$ structural models (with $\frac{1}{8}$ ML C). The surface energy of the 2RD model is used as a reference.

Model	ΔE (Present work)	ΔE (Ref. 4)
rMD	0.13	0.11
rMD_β	0.79	0.77
2RD	0.00	0.00
$\mathrm{2RD}_\beta$	0.06	0.04
1RD	−0.25	
1RD′	−0.09	
2RD′	0.02	

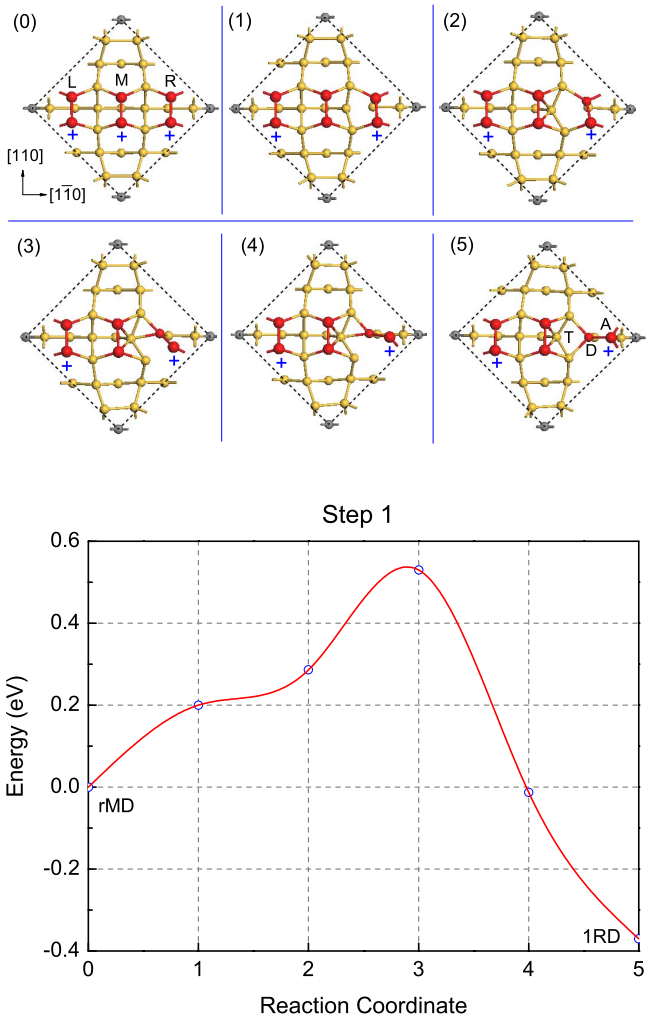

FIG. 2. (Color online) The snapshots (top views) of the reaction process at step 1 along Path I (upper panel). The rMD model was transformed to the 1RD model via dimer rotation at this step. The energy profile of this reaction is shown in the lower panel. The zero energy is defined by that of the rMD model. The data points are fitted with a cubic spline. The migration energy barrier is 0.53 eV. In the saddle point [image (3)], the right Si dimer rotated by about 45° counterclockwise.

(toward or away from, respectively). To obtain the reaction pathways and estimate the diffusion barrier heights between the rMD and 2RD configurations, we performed NEB calculations.[27,28] Adequate intermediate structures (images) between the rMD and 2RD configurations were interpolated based on the different dimer rotation paths, which were used as starting guesses for NEB calculations.

For the dimer rotation along Path I, we found that the reaction process involved four steps. First, the right Si dimer of the rMD model rotated counterclockwise by 90°, while the left Si dimer was almost frozen during this step. The snapshots and energy profile of the reaction at this step are shown in Fig. 2. As clearly seen in image (3) of Fig. 2, the right Si dimer rotated about 45° counterclockwise to reach the saddle point. The energy barrier of this step is 0.53 eV, as shown in the energy profile of Fig. 2. It is interesting to note that at this step the rMD changed to a new stable structure [image (5) in Fig. 2] with a single rotated dimer. This new structure is more stable than the 2RD model by 0.25 eV per $c(4\times4)$ cell. In this structure, the lower atom of the rotated dimer [atom D labeled in image (5) of Fig. 2] is low enough (1.47 Å lower than the upper one) to form a bond with a fourth layer Si atom [referred to as atom F, see Fig. 5(a)] directly below it and its dangling bond is saturated. The fourth layer Si atom F pushed away one of its neighboring Si atoms in the third layer [atom T labeled in image (5) of Fig. 2] toward the middle Si dimer. Due to the approach of Si atom T, the middle Si dimer was almost flattened. We will refer to this new structure as the 1RD model thereafter and discuss it in more detail in next subsection.

At the second step, the lower atom of the rotated dimer, atom D, raised while the higher atom of the rotated dimer lowered. The tilt direction of the nonrotated left dimer was also reversed at this step. The bond between atom D and the fourth layer Si atom F was broken. As a result, the third layer Si atom T returned to its original place in the rMD model [see image (10) in Fig. 3]. We named the structure (10) as the 1RD′ model. This model is characterized with one-half unit cell resembling the 2RD model and the other half remaining the configuration in the rMD model. The 1RD′ structure is energetically unfavorable than 1RD, but still 0.09 eV more stable than 2RD, as listed in Table I.

At the third step, the left dimer rotated clockwise by 90° and the lower Si atom of the left rotated dimer lowered to bond with the fourth layer Si atom directly below it. The dimer rotation process is very similar to that of the right dimer in the first step. The fully relaxed structure of the final state of this step is shown in image (15) of Fig. 3 (referred to as the 2RD′ model hereafter). Note that one-half of the 2RD′ model is similar to the 1RD model, while the other half resembles the 2RD model. The 2RD′ model is slightly (0.02 eV) less stable than 2RD. The relative surface energies of all models are listed in Table I for reference. At the fourth step, the lower atom of the left rotated dimer of the 2RD′ model raised and brought the surface to the 2RD model.

The snapshots of the reaction processes and energy profile from steps 2 to 4 are shown in Fig. 3. Summarized in Table II are the energy barriers for the aforementioned four steps. The whole reaction processes along Path I is rMD→1RD →1RD′→2RD′→2RD. As seen in Table II and Fig. 3, the rate-limiting reaction process along Path I is the dimer rotation at the third step, namely, 1RD′→2RD′. The overall energy barrier from rMD to 2RD along Path I is 0.82 eV.

We plotted the variation of height difference between two Si atoms, d_h, of the three Si dimers during the whole reaction along Path I in Fig. 4. At step one (rMD→1RD), the d_h of the right dimer (which rotated at this step) increased, while the d_h of the left dimer showed little variation. At the second step (1RD→1RD′), the d_h of both the left and right dimers decreased. The tilt direction of the left dimer was reversed after reaction coordinate 8, as shown by the negative d_h of the left dimer in Fig. 4. At step three (1RD′→2RD′), the d_h of the left dimer (which rotated at this step) increased and the original tilt direction was restored. The right dimer was almost kept frozen, as shown by the little variation of its d_h. At the last step (2RD′→2RD), the d_h of the left dimer de-

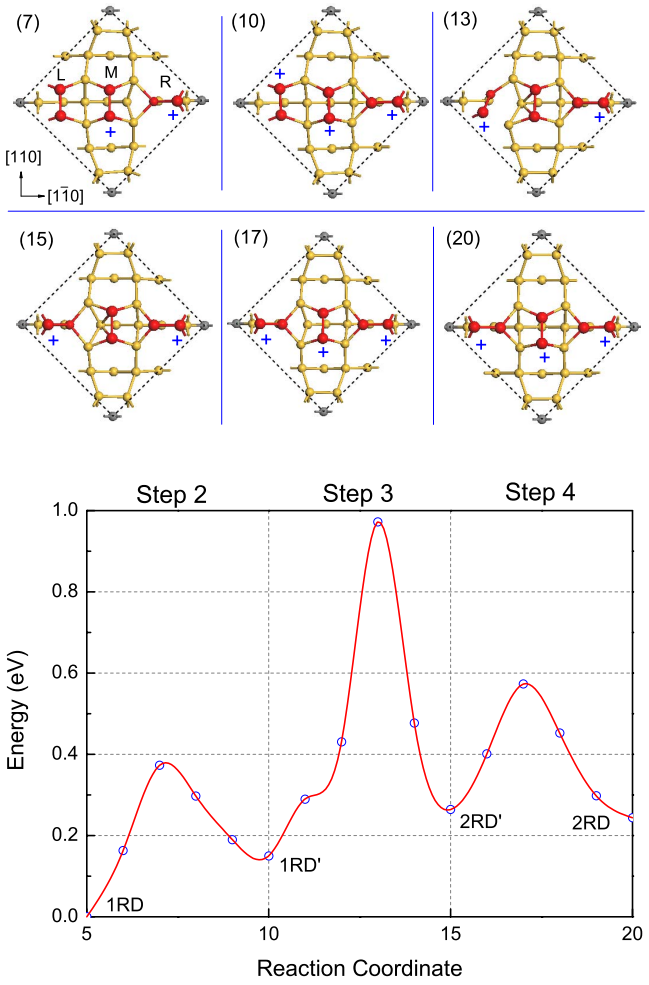

FIG. 3. (Color online) The snapshots (top views of six selected images) of the reaction processes from steps 2 to 4 along Path I. The 1RD structure was transformed to 2RD via dimer rotation or raise (upper panel), by passing through two intermediate structures, 1RD′ and 2RD′. The energy profile of these reaction processes is shown in the lower panel. The zero energy is defined by that of the 1RD model. The data points are fitted with a cubic spline. The dimer rotation in 1RD′→2RD′ is the rate-limiting process. The overall energy barrier is 0.82 eV.

creased while that of the right dimer increased slightly. It is interesting to note that during dimer rotations, the d_h of the middle dimer showed a large variation, although the middle dimer did not rotate at all in the reaction. As clearly shown in Fig. 4, the d_h of the middle dimer in rMD (0.46 Å) was much smaller than that of the clean Si(001)-$p(2\times2)$ surface (0.75 Å in our calculation). It almost vanished in the 1RD and 2RD′ models, and peaked in the 1RD′ and 2RD models.

The reaction process along Path II can be divided into two steps. First, the right Si dimer rotated clockwise by 90° and transformed the rMD model to the 1RD′ model directly, without passing through the 1RD state. The energy barrier of this step is 1.10 eV. Next, the left dimer of the 1RD′ rotated counterclockwise by 90° and changed the surface structure to 2RD directly with an energy barrier of 1.26 eV. The overall energy barrier from the rMD to 2RD along Path II is

TABLE II. Energy barriers (E_a) for different pathways of Si dimer rotations on the C-induced Si(001)-$c(4\times4)$ surface, see Fig. 1. L or R indicates which dimer (Left or Right) is moving. Two dimer rotation directions are possible, clockwise (CW) or counterclockwise (CCW). UP indicates the raise of the dimer.

Paths	Steps	Movement	E_a (eV)
I	rMD→1RD	R-CCW	0.53
	1RD→1RD′	R-UP	0.37
	1RD′→2RD′	L-CW	0.82
	2RD′→2RD	L-UP	0.31
II	rMD→1RD′	R-CW	1.10
	1RD′→2RD	L-CCW	1.26
III	rMD→1RD	L-CW	0.53
	1RD→1RD′	L-UP	0.37
	1RD′→2RD	R-CW	1.26

1.26 eV, 0.44 eV higher than that of the reaction process along Path I.

The dimer rotation along Path III consists of three steps. First of all, the left dimer rotated clockwise by 90° and the lower Si atom of the left rotated dimer lowered to bring the rMD to the 1RD structure. This step is similar to step 1 in Path I, where the right dimer rotated instead. Next, the lower atom of the left rotated dimer raised and the 1RD model was transformed to the 1RD′ model. This process is also symmetric to that at step two in Path I. Finally, the right dimer of the 1RD′ model rotated clockwise by 90° and changed the surface to the 2RD model. This step is identical to the second step in Path II. The overall energy barrier along Path III is also 1.26 eV.

From the reaction processes along different pathways, we can conclude that the energy barrier for the structural transformation from the rMD model to the 2RD model is sensitive to the directions of the rotation of Si dimers. The mini-

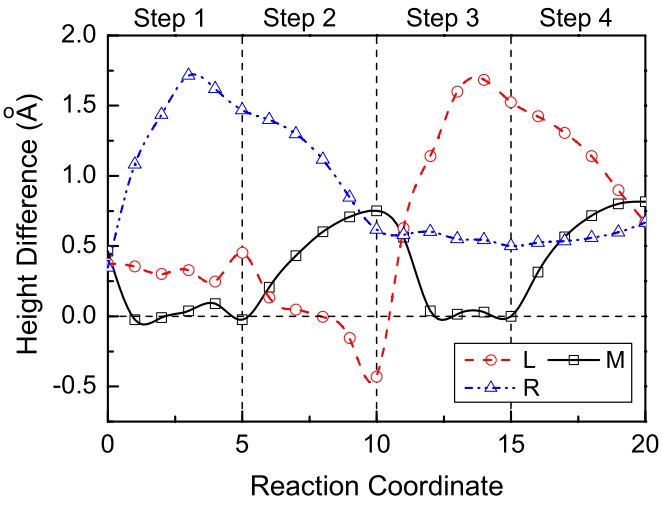

FIG. 4. (Color online) The height difference between two Si atoms, d_h, of the left dimer (L), middle dimer (M), and right dimer (R) versus the reaction coordinate for the reaction along Path I. The data points are fitted with a cubic spline.

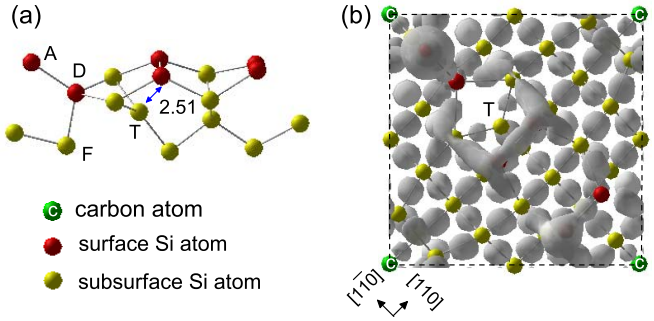

FIG. 5. (Color online) (a) A bird's eye view of the 1RD model. (b) The isosurface of ELF for the 1RD model at the value 0.82.

mum energy path is Path I, namely, the two side dimers rotate toward the middle dimer by 90°, with a rotational barrier of 0.82 eV. The energy barriers of Paths II and III are relatively higher, 1.26 eV. The values of all relative energy barriers can be found in Table II. The low energy barrier suggests that the dimer rotation on the C-induced Si(001)-$c(4\times4)$ surface is fast, and comparable to the Si ad-dimer rotation on the Si(001) surface (with 0.70 eV rotational barrier).[29,30]

C. A new stable 1RD model

A new structure, 1RD, was found to be more stable than the previously most stable 2RD model by 0.25 eV per $c(4\times4)$ cell. It plays an important role in the dimer rotation on the C-induced Si(001)-$c(4\times4)$ surface. In this structure, the lower atom of the rotated dimer, atom *D*, is bonded with a fourth layer Si atom [labeled *F* in Fig. 5(a)] directly below it and the dangling bond of atom *D* is saturated [see Fig. 5(a)]. As a result, the higher Si atom of the rotated dimer [atom *A* labeled in Fig. 5(a)] is left behaving like an adatom. The bond between atom *T* and atom *F* is broken. And atom *T* approaches to the middle dimer. As a result, the middle dimer is leveled. The distances between the two Si atoms of the middle dimer and atom *T* are both 2.51 Å. However, the analysis of the nature of bonding by employing the electron localization function (ELF) (Ref. 31), reveals that atom *T* does not form bonds with either Si atom of the middle dimer [see Fig. 5(b)]. Si atom *T* is threefold coordinated and shows sp^2-like hybridization characteristics. The stabilization mechanism of the 1RD model could be ascribed to the annihilation of one surface dangling bond and the formation of an sp^2-like bonding in the subsurface.

By an analog of the three possible phases of the Si(001) surface, i.e., $p(2\times1)$, $p(2\times2)$, and $c(4\times2)$, we investigate the ordering of the 1RD model in a larger supercell. For this purpose, we prepared a $c(8\times8)$ supercell, where four 1RD units were embedded. There are three possible ways to include four 1RD units into the $c(8\times8)$ supercell: (i) all 1RD units being in phase, (ii) each two 1RD units in the same dimer rows being 180° out of phase, and (iii) each 1RD unit being 180° out of phase with its neighboring units. Each configuration has been fully relaxed using Γ sampling only. Our calculations show that configuration (iii) is energetically more favorable than configuration (i) by 0.04 eV per $c(4\times4)$ cell, while configuration (ii) is less stable by 0.15 eV per $c(4\times4)$ cell. The optimized structure of configuration (iii) is shown in Fig. 6. The small energy difference in configurations (i) and (iii) suggests that these two configurations could coexist and both may be observed in experiments.

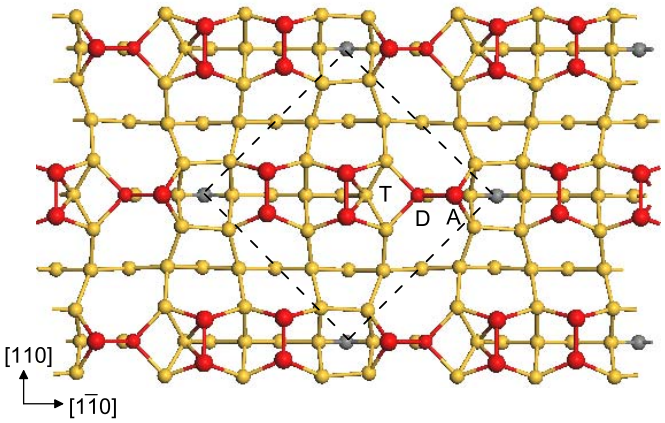

FIG. 6. (Color online) Schematic diagram of the 1RD model in a larger $c(8\times8)$ supercell, with each 1RD unit being 180° out of phase with its neighboring units. The embedded $c(4\times4)$ 1RD unit is indicated by the dashed line.

D. A possible method to search for new stable structures

Finally, we would like to propose a possible method to search for new stable structures based on the existing models. Assume that the existing models are very close in geometry and contain identical elements. If these models could be transformed to one another by reactions, say, diffusion, one could map out the reaction paths in the phase configuration by NEB calculations. If the energy profile drops to valleys along the reaction paths, then the intermediate structures could be more stable than the initial and/or final states. If one can pick out the constrainedly relaxed intermediate structures and fully relax them, then chances there are to find new stable or metastable structures. The identification of 1RD, 1RD′, and 2RD′ models above is an example. We expect that this method could be found useful in future work.

IV. CONCLUSIONS

In conclusion, we presented results of first-principles calculations on possible reaction pathways for Si dimer rotation on the C-induced Si(001)-$c(4\times4)$ surface. We showed that the 2RD model could be obtained from the rMD model by dimer rotation. The energy barrier was found to be sensitive to the rotation directions of Si dimers. The minimum energy path from rMD to 2RD was the rotations of two side dimers toward the middle dimer, with a 0.82 eV energy barrier. This reaction pathway passed through three stable configurations, the 1RD, 1RD′, and 2RD′ models. The 1RD model was found to be more stable than all existing models and its

energy was lower than that of the 2RD model, the previously most stable structure, by 0.25 eV per $c(4\times4)$ unit cell. The stabilization of the 1RD model could be understood by the effect of the annihilation of one surface dangling bond and the formation of an sp^2-like bonding in the subsurface. We expected that this model could be observed in experiment, such as by using low temperature STM. Finally, a possible method to search for new stable structures based on the existing models by mapping out the reaction paths in the phase configuration was proposed.

*Electronic address: phyfyp@nus.edu.sg

[1] H. Rücker, M. Methfessel, E. Bugiel, and H. J. Osten, Phys. Rev. Lett. **72**, 3578 (1994).
[2] J. Tersoff, Phys. Rev. Lett. **74**, 5080 (1995).
[3] W. Kim, H. Kim, G. Lee, and J.-Y. Koo, Phys. Rev. Lett. **89**, 106102 (2002).
[4] H. Kim, W. Kim, G. Lee, and J.-Y. Koo, Phys. Rev. Lett. **94**, 076102 (2005).
[5] R. N. Thomas and M. H. Francombe, Appl. Phys. Lett. **11**, 108 (1967).
[6] T. Sakamoto, T. Takahashi, E. Suzuki, A. Shoji, H. Kawanami, Y. Komiya, and Y. Tarui, Surf. Sci. **86**, 102 (1979).
[7] R. I. G. Uhrberg, J. E. Northrup, D. K. Biegelsen, R. D. Bringans, and L.-E. Swartz, Phys. Rev. B **46**, 10251 (1992).
[8] J. Y. Maeng and S. Kim, Surf. Sci. **482-485**, 1445 (2001).
[9] L. Li, C. Tindall, O. Takaoka, Y. Hasegawa, and T. Sakurai, Phys. Rev. B **56**, 4648 (1997).
[10] L. Simon, M. Stoffel, P. Sonnet, L. Kubler, L. Stauffer, A. Selloni, A. De Vita, R. Car, C. Pirri, G. Garreau, D. Aubel, and J. L. Bischoff, Phys. Rev. B **64**, 035306 (2001).
[11] Y. Wang, R. J. Hamers, and E. Kaxiras, Phys. Rev. Lett. **74**, 403 (1995).
[12] H. Nörenberg and G. A. D. Briggs, Surf. Sci. **430**, 154 (1990).
[13] K. Miki, K. Sakamoto, and T. Sakamoto, Appl. Phys. Lett. **71**, 3266 (1997).
[14] O. Leifeld, D. Grützmacher, B. Müller, K. Kern, E. Kaxiras, and P. C. Kelires, Phys. Rev. Lett. **82**, 972 (1999).
[15] I. N. Remediakis, E. Kaxiras, and P. C. Kelires, Phys. Rev. Lett. **86**, 4556 (2001).
[16] C.-L. Liu, L. J. Borucki, T. Merchant, M. Stoker, and A. Korkin, Appl. Phys. Lett. **76**, 885 (1999).
[17] C.-L. Liu, L. Borucki, T. Merchant, M. Stoker, and A. Korkin, Phys. Rev. B **62**, 5021 (2000).
[18] Ph. Sonnet, L. Stauffer, A. Selloni, A. De Vita, R. Car, L. Simon, M. Stoffel, and L. Kubler, Phys. Rev. B **62**, 6881 (2000).
[19] Ph. Sonnet, L. Stauffer, A. Selloni, and A. De Vita, Phys. Rev. B **67**, 233305 (2003).
[20] J. R. Ahn, H. S. Lee, Y. K. Kim, and H. W. Yeom, Phys. Rev. B **69**, 233306 (2004).
[21] S. T. Jemander, H. M. Zhang, R. I. G. Uhrberg, and G. V. Hansson, Phys. Rev. B **65**, 115321 (2002).
[22] G. Kresse and J. Furthmüller, Phys. Rev. B **54**, 11169 (1996).
[23] G. Kresse and J. Furthmüller, Comput. Mater. Sci. **6**, 15 (1996).
[24] D. Vanderbilt, Phys. Rev. B **41**, R7892 (1990).
[25] J. P. Perdew and Y. Wang, Phys. Rev. B **45**, 13244 (1992).
[26] H. J. Monkhorst and J. D. Pack, Phys. Rev. B **13**, 5188 (1976).
[27] G. Henkelman, B. P. Uberuaga, and H. Jónsson, J. Chem. Phys. **113**, 9901 (2000).
[28] G. Henkelman and H. Jónsson, J. Chem. Phys. **113**, 9978 (2000).
[29] B. S. Swartzentruber, A. P. Smith, and H. Jónsson, Phys. Rev. Lett. **77**, 2518 (1996).
[30] B. Borovsky, M. Krueger, and E. Ganz, Phys. Rev. Lett. **78**, 4229 (1997).
[31] B. Silvi and A. Savin, Nature (London) **371**, 683 (1994).